Quantum phase transition in a multicomponent Bose-Einstein condensate in optical lattices

Guang-Hong Chen and Yong-Shi Wu

Department of Physics, University of Utah, Salt Lake City, Utah 84112

We present a general lattice model for a multicomponent atomic Bose-Einstein system in an optical lattice. Using the model, we analytically study the quantum phase transition between the Mott insulator and a superfluid. A mean-field theory is developed from the Mott-insulator ground state. When the interspecies interactions are strong enough, the Mott insulator demonstrates the phase separation behavior. For weak interspecies interactions, the multispecies system is miscible. Finally, the phase diagram is discussed with emphasis on the role of interspecies interactions. The tip and the shape of the Mott insulator lobes do not depend on the interspecies interactions, but the latter indeed modify the position of the phase boundaries.

I. INTRODUCTION

The study of quantum phase transitions (QPT) has attracted much interest in recent years [1,2]. The term "quantum" is used to emphasize that it is the quantum fluctuations that play a vital role in driving the transition from one phase to another. In contrast, the usual thermodynamic phase transition at finite temperature is driven by thermal fluctuations, which are experimentally controlled by tuning the temperature of the system. As temperature is lowered, the thermal fluctuations are suppressed and finally they are not strong enough to drive a finite-temperature phase transition. However, this by no means implies that there would be no phase transition at very low temperature, since quantum fluctuations still exist and they may be sufficiently strong to drive a phase transition even at zero temperature. We call such a zero-temperature phase transition a QPT, and it is experimentally accessible by tuning parameters of the system other than temperature.

Several prominent examples have been extensively studied to demonstrate QPT. One example is quantum Hall (QH) systems, where different QH phases can be achieved by tuning either the magnetic field or the carrier concentration [1]. The second example is a network of Josephson junctions [3]. A Josephson junction is a tunnel junction connecting two superconducting metallic grains. A Cooper pair of electrons is able to tunnel back and forth between the grains. If the Cooper pairs can move freely from grain to grain in the network, the system is superconducting. However, since the grains are very small, it costs a charging energy to move a Cooper pair to neighboring grains. When the charging energy is big enough, the Cooper pairs fail to propagate among the grains and the network will be in an insulating phase.

A third system that exhibits QPT involves the superfluid ^{4}He. When the superfluid ^{4}He is absorbed in the porous media or on different substrates, the bosonic atoms in ^{4}He experience external forces from the other medium. When the interactions between atoms are much weaker than the above external forces, the system is expected to be a superfluid. In the opposite limit, the superfluid phase cannot be maintained, and the system will exhibit a Mott-insulator behavior. Thus a superfluid–Mott-insulator phase transition is expected to happen, if one can tune the strength of atomic interactions.

Detailed discussions can be found in Ref. [4] by Fisher and co-workers. The starting point is the following boson-Hubbard model:

$$H = -J \sum_{\langle i,j \rangle} (a_i^\dagger a_j + \text{H.c.}) + \sum_i \varepsilon_i n_i + \frac{U}{2} \sum_i n_i(n_i - 1). \quad (1)$$

Here a_i and $a_i^\dagger$ correspond to the bosonic annihilation and creation operators on the ith lattice site, $n_i = a_i^\dagger a_i$ is the atomic number operator on the ith site, and ε_i the energy offset of the atom on the ith site due to external harmonic confinement. The last term corresponds to the on-site repulsion between atoms, while the first term describes the tunneling of atoms between neighboring sites. At mean-field level, starting with a strong-coupling expansion, namely, treating the hopping term as a perturbation, the system is found to have a QPT at the following critical value [4–7] for the ratio U/J:

$$\frac{U}{J} = z n_0, \quad (2)$$

where $z = 2d$ for a d-dimensional simple lattice and n_0 is the inverse fraction of condensed atoms in a canonical ensemble. For instance, $n_0 \approx 5.83$ for the three-dimensional case.

Experimentally, such critical point of QPT is very hard to access. Temperature is an annoying factor for a convincing demonstration of the QPT: The intrusion of thermal fluctuations often washes out the effects of quantum fluctuations. This makes the temperature window to observe the QPT small. Moreover, to make the system cross the quantum critical point, we need to tune the controlling parameter carefully. In most of the studied cases, this is hard to manipulate. Even if one can tune the parameter, the range of tunability is normally very small. Until very recently, in most cases only the magnetic field [1,8] is the tunable parameter. Finally, the presence of disorder makes the observation of QPT even more difficult.

Recently Ref. [9] reported the success in realizing a superfluid–Mott-insulator phase transition in a gas of ultracold atoms in an optical lattice. This is a revolutionary breakthrough for the experimental observation of a controllable

QPT. They cooled the atomic gas of ^{87}Rb down to 10 nK to realize the atomic Bose-Einstein condensation (BEC). Moreover, the BEC is loaded into a perfect, simple-cubic, optical lattice formed by six criss-cross laser beams. By controlling the intensity of the laser beams, they can efficiently control the potential height of the above simple-cubic lattice in a very large range. In addition, such a unique invention of the artificial lattice has the great advantage that the system is basically defect-free. By using this setup, they successfully and repeatedly observed the QPT at the critical value given by Eq. (2). Thus an ideal playground for QPT has been created in the atomic BEC system, which provides us an opportunity to test many theoretical predictions.

A significant difference between the atomic BEC superfluid and the ^{4}He superfluid is that the former allows atoms to condense with different internal states due to hyperfine splitting. This allows the order parameter of the superfluid to possess a larger symmetry than the familiar U(1) [10,11]. It is referred to in the BEC community as a spinor BEC. As pointed out by Ho [10,11] and many others [12,13], the spinor BEC possesses a whole host of quantum phenomena that are absent in the scalar cases: For instance, vector and quadrupolar spin-wave modes, Skyrmions, and other quantum orders, etc. Experimentally, one can condense different matter species into one single internal state and study the effects of cross-species interactions. Throughout this paper, we would like to call such systems as multicomponent BEC systems.

In the Mott insulator to superfluid quantum phase transition, quantum fluctuations and atomic interactions play a vital role. Without interactions, one has only the so-called band insulator. In the atomic gas, due to laser cooling technology, BEC can be realized simultaneously in several internal hyperfine levels [14]. This makes the experimental study of the multicomponent BEC possible. Among all the interesting physics discovered in the multicomponent BEC, the interspecies repulsive interactions play a very important role. Therefore, it would be very interesting to study how interspecies interactions affect the transition from the Mott insulator to the superfluid.

Motivated both by the experimental progress and by theoretical curiosity, we shall study in the present paper the superfluid–Mott-insulator transition in a multicomponent BEC system in the presence of a periodic potential created by criss-cross laser beams. The layout of the paper is the following: In Sec. II the multispecies boson-Hubbard model is derived for the general case and for several special cases as well. In Sec. III, we study the ground state and its stability in the strong-coupling limit. The phase boundary between the superfluid and the Mott insulator is determined for the two-component case in Sec. IV, while Sec. V is devoted to the presentation of a schematic phase diagram. Finally, we summarize our results in Sec. VI.

II. THE MODEL

A. The general boson-Hubbard model for a multicomponent BEC

After including the optical lattice potential, the most general model Hamiltonian for a multicomponent boson gas can be written, in the second-quantization notations, as

$$H = \int d^3x \left[\psi_i^\dagger(x) \left(-\frac{\hbar^2\nabla^2}{2m_a}\delta_{ij} + U_{ij}(x) + V_i(x)\delta_{ij} \right) \psi_j(x) + \frac{g_{ij,kl}}{2} \psi_i^\dagger(x)\psi_j^\dagger(x)\psi_k(x)\psi_l(x) \right],$$

$$(3)$$

where m_a is the mass of an individual atom, the indices i,j,k,l label the components of the atoms, and the summation is assumed for repeated indices. Generically we allow the external potential U_{ij} to have a nondiagonal part in the hyperfine spin basis, in which it represents a Josephson-type coupling between spin components [15]. $V_i(x)$ denotes the optical lattice potential seen by the atoms of species i. For the experimental configuration in Ref. [9], this lattice is modeled by

$$V(x,y,z) = V_0(\sin^2 kx + \sin^2 ky + \sin^2 kz), \qquad (4)$$

with k is the wave vector of the laser light and V_0 is the depth of the potential well. In the multicomponent case, the depth $V_{0,i}$ may depend on the species index i. The interatomic interactions in Eq. (3) have been approximated as a contact interaction in which the coefficients $g_{ij,kl}$ describe the strength of various elastic and inelastic collisions.

For a single atom in the trap and the periodic potential, the energy eigenstates are Bloch states. In the tight-binding limit, we can superpose the Bloch states to get a set of Wannier functions that are localized on individual lattice sites. Within the single-band approximation, we can expand the field operators in the Wannier basis as

$$\psi_i(x) = \sum_n b_{ni} w_i(x - x_n), \qquad (5)$$

where $w_i(x-x_n)$ is the Wannier function around lattice site n. Using Eq. (5), the general Hamiltonian (3) is reduced to a generalized boson-Hubbard Hamiltonian for the multicomponent BEC:

$$H = -\sum_{\langle m,n\rangle} J_{mn}^{ij}(b_{mi}^\dagger b_{nj} + \text{H.c.}) + \sum_m \varepsilon_{mi} b_{mi}^\dagger b_{mi} + \frac{U_{ij,kl}}{2}\sum_m b_{mi}^\dagger b_{mj}^\dagger b_{mk} b_{ml}.$$

$$(6)$$

Here J_{mn}^{ij} is the hopping matrix element between two adjacent lattice sites m and n. It is defined by

$$J_{mn}^{ij} = -\int d^3x\, w_i^*(x - x_m) \left[-\frac{\hbar^2\nabla^2}{2m_a}\delta_{ij} + V_i\delta_{ij} + U_{ij} - \frac{1}{2}(U_{ii} + U_{jj}) \right] w_j(x - x_n).$$

$$(7)$$

Within the Hubbard approximation, the hopping integral is lattice site independent, i.e., $J_{mn}^{ij} \approx J^{ij}$. ε_{ni} describes the energy offset on each site due to the trap confinement. It is defined as

$$\varepsilon_{ni} = \int d^3x \, U_{ii}(x) |w_i(x-x_n)|^2. \tag{8}$$

(Here we only consider the lowest band in the optical lattice, whose bottom is taken to be the zero point for energy.) Finally, to get the on-site interactions in Eq. (6), the Hubbard approximation has been used to approximate the multicenter integral as a single-center one; namely, we have

$$
\begin{aligned}
U_{ij,kl} &= g_{ij,kl} \int d^3x \, w_i^*(x-x_{n1}) w_j^*(x-x_{n2}) \\
&\quad \times w_k(x-x_{n3}) w_l(x-x_{n4}) \\
&\approx g_{ij,kl} \int d^3x \, w_i^*(x) w_j^*(x) w_k(x) w_l(x).
\end{aligned} \tag{9}
$$

The general form of the boson-Hubbard model (6) contains a large number of parameters. In the following, we would like to discuss several special cases that might be relevant to experiments. The first simple case is, of course, given by Eq. (1) for a single component BEC. It was first derived and studied in the context of atomic BEC in Ref. [16].

B. Two-component boson-Hubbard model

The second example we will discuss is the two-component BEC. Experimentally, the simultaneous condensation of ^{87}Rb atoms in the two internal states ($F=2, M=2$) and ($F=2, M=-1$) has been accomplished by Myatt *et al.* [17]. For this case, we discuss Bose condensed atoms with two internal hyperfine levels $|A\rangle$ and $|B\rangle$. The atoms interact only through the following three channels: AA-, BB-, and AB-type elastic collisions. Then our Hamiltonian (6) is reduced to

$$
\begin{aligned}
H_2 &= -\sum_{\langle m,n\rangle} [J^A b_{mA}^\dagger b_{nA} + J^B b_{mB}^\dagger b_{nB} + J^{AB} b_{mA}^\dagger b_{nB} + \text{H.c.}] \\
&\quad + \sum_m (\varepsilon_{mA} n_{mA} + \varepsilon_{mB} n_{mB}) + \frac{1}{2}\sum_m [U_A n_{mA}(n_{mA}-1) \\
&\quad + U_B n_{mB}(n_{mB}-1) + 2U_{AB} n_{mA} n_{mB}].
\end{aligned} \tag{10}
$$

A similar energy-level and interaction pattern has been discussed by another group in a different context [18]. To be concrete, we focus on the situation in which the trap potential is diagonal in internal space, namely, U_{ij} only have diagonal components U_{ii}. In this case, it follows from Eq. (7) that

$$J_{mn}^{AB} = 0. \tag{11}$$

To get more insight into the parameters in Eq. (10), we have to use the explicit form of the Wannier functions. To do so, we notice that the optical lattice potential is sinusoidal. The Wannier function could be constructed as the localized one determined by the following eigenvalue problem:

$$\left[\frac{P^2}{2m_a} + V(x,y,z)\right]\phi(x,y,z) = E\phi(x,y,z). \tag{12}$$

The lattice sites are given by the minima of the lattice potential $V(x,y,z)$; around them the potential V is approximately quadratic:

$$V(x,y,z) \approx \tfrac{1}{2} m_a \omega (x^2 + y^2 + z^2), \tag{13}$$

where ω is given by

$$\omega = 2m_a k^2 V_0. \tag{14}$$

(Here, for simplicity, we assume that the depth of the optical potential is the same for different species; it is straightforward to generalize our results to the case with $V_0 \to V_{0,i}$ dependent on the species index i.) Therefore, within the single-band approximation, the Wannier function is approximately given by the ground-state wave function of a three-dimensional harmonic oscillator. Namely,

$$w_{A/B} = \left(\sqrt{\frac{\alpha}{\sqrt{\pi}}}\right)^3 \exp\left[-\frac{1}{2}\alpha^2(x^2+y^2+z^2)\right], \tag{15}$$

where $\alpha = \sqrt{m_a \omega/\hbar}$. Noting that the Wannier functions are independent of species indices within our approximations. Thus we can take

$$J_A = J_B = J. \tag{16}$$

Finally, the on-site energy is the original interatomic interaction with an extra numerical factor $\int [w(x,y,z)]^4$. Therefore, the Hamiltonian (10) can be cast into

$$
\begin{aligned}
H_2 &= -J\sum_{\langle m,n\rangle} (b_{mA}^\dagger b_{nA} + b_{mB}^\dagger b_{nB} + \text{H.c.}) \\
&\quad + \sum_m (\varepsilon_{mA} n_{mA} + \varepsilon_{mB} n_{mB}) + \frac{1}{2}\sum_m [U_A n_{mA}(n_{mA}-1) \\
&\quad + U_B n_{mB}(n_{mB}-1) + 2U_{AB} n_{mA} n_{mB}].
\end{aligned} \tag{17}
$$

Our Hamiltonian (17) is different from the two-species boson-Hubbard model proposed in Ref. [16], where the authors assumed that two species A and B are placed in two different optical lattices with a relative half-period shift. Also a drive laser has been applied to induce a transition between species A and B. In this situation, J^A and J^B in Eq. (10) should be neglected since they represent the next-nearest-neighbor hopping. Moreover, the on-site mutual interactions between two species are of higher orders compared with the on-site interactions for the same species. In this way, we recover their Hamiltonian [16]

$$\tilde{H}_2 = -J \sum_{\langle m,n \rangle} (b_{mA}^{\dagger} b_{nB} + \text{H.c.}) + \sum_m (\varepsilon_{mA} n_{mA} + \varepsilon_{mB} n_{mB})$$

$$+ \frac{1}{2} \sum_m [U_A n_{mA}(n_{mA}-1) + U_B n_{mB}(n_{mB}-1)$$

$$+ 2U_{AB} n_{mA} n_{mB}]. \tag{18}$$

C. Boson-Hubbard model for the spinor BEC

Another well-studied example of the multicomponent BEC is the so-called spinor BEC [11,15]. For a system of spin $f = 1$ bosons, such as ^{23}Na, ^{39}K, and ^{87}Rb atoms, the form of the interatomic interactions is largely constrained by symmetries. In this case, the number of the interaction parameters is reduced to two. The interaction potential can be written as

$$V_{int}(x_1, x_2) = (g_0 + g_2 \vec{F}_1 \cdot \vec{F}_2) \delta(x_1 - x_2), \tag{19}$$

where the parameters g_0 and g_2 are defined by the scattering lengths a_2 and a_0 as

$$g_0 = \frac{4\pi\hbar^2}{m_a} \frac{2a_2 + a_0}{3}, \tag{20}$$

$$g_2 = \frac{4\pi\hbar^2}{m_a} \frac{a_2 - a_0}{3}. \tag{21}$$

To facilitate the discussion, we choose a basis to make the trapping potential U_{ij} in Eq. (3) diagonal. Thus the hopping integral is nonvanishing only between the same species. In addition, the on-site interactions are reduced to the following eight terms:

$$H_{int} = \frac{1}{2} \sum_{mA} U_A n_{mA}(n_{mA}-1) + \frac{1}{2} \sum_{m,A \neq B} U_{AB} n_{mA} n_{mB}$$

$$+ \frac{U_0}{2} \sum_m (b_{m0}^{\dagger 2} b_{m1} b_{m\bar{1}} + \text{H.c}). \tag{22}$$

Here the species index $A = 1, 0, \bar{1} (= -1)$. U_A, U_{AB}, and U_0 are determined by the parameters g_0, g_2 and the Wannier functions. In particular, the parameter U_0 is proportional to g_2. Moreover, g_2 is determined by the difference between scattering lengths as shown in Eq. (21). For the sodium case, the difference between the two scattering lengths is very small (0.29 nm) compared with $2a_2 + a_0 = 7.96$ nm. Therefore, $g_2 \ll g_0$ so that we can neglect the spin-relaxation channel in the interaction terms. Namely, we set $U_0 = 0$ as the zeroth-order approximation. Within this approximation, we get the following boson-Hubbard model for a spin-1 spinor BEC, when it is loaded into the optical lattice potential:

$$H_3 = -\sum_{\langle m,n \rangle A} (J^A b_{mA}^{\dagger} b_{nA} + \text{H.c.}) + \sum_{mA} \varepsilon_{mA} n_{mA}$$

$$+ \frac{1}{2} \sum_{mA} U_A n_{mA}(n_{mA}-1) + \frac{1}{2} \sum_{m,A \neq B} U_{AB} n_{mA} n_{mB}. \tag{23}$$

In the following section, we will discuss the possible mean-field phase diagram for the superfluid–Mott-insulator phase transition by starting with the two-component boson-Hubbard Hamiltonian (10).

III. MOTT GROUND STATE AND ITS STABILITY

We are going to employ the strong coupling expansion to develop a mean-field theory. In the strong-coupling limit, the hopping term can be treated as a perturbation. In the zeroth-order approximation, we ignore it for a while. The Hamiltonian is then decoupled for the site index. The ground state is given by the occupation number state $|n_A, n_B\rangle$, with the wave function

$$|\text{ground}\rangle_{MF} \sim \prod_m (b_{mA}^{\dagger})^{n_A} (b_{mB}^{\dagger})^{n_B} |0\rangle. \tag{24}$$

To get the ground-state energy, we need to minimize the energy at each site (for this purpose, we neglect the site index in the following discussions); namely, we need to minimize the energy function $E(n_A, n_B)$ given by

$$E(n_A, n_B) = \varepsilon_A n_A + \varepsilon_B n_B + \frac{1}{2}[U_A n_A(n_A-1) + U_B n_B(n_B-1)$$

$$+ 2U_{AB} n_A n_B]. \tag{25}$$

If we skip over the fact for the moment that the occupation number n_A and n_B are integers, then the conditions to minimize the above energy function are given by

$$U_A n_A + U_{AB} n_B = \frac{U_A}{2} - \varepsilon_A, \tag{26}$$

$$U_{AB} n_A + U_B n_B = \frac{U_B}{2} - \varepsilon_B. \tag{27}$$

Solving the two coupled linear equations, we get

$$n_A = \frac{U_B(U_A - U_{AB}) + 2(\varepsilon_B U_{AB} - \varepsilon_A U_B)}{2(U_A U_B - U_{AB}^2)}, \tag{28}$$

$$n_B = \frac{U_A(U_B - U_{AB}) + 2(\varepsilon_A U_{AB} - \varepsilon_B U_A)}{2(U_A U_B - U_{AB}^2)}. \tag{29}$$

Now we take care of the fact that the occupation numbers must be integer. So the actual numbers to minimize the energy are the two integers closest to the above $n_{A/B}$. To do so, we can write $n_{A/B}$ in terms of the closest integer numbers $n_{A/B}^0$ and the decimal parts, i.e.,

$$n_A = n_A^0 + \alpha, \quad n_B = n_B^0 + \beta, \tag{30}$$

where the numbers α and β satisfy

$$-\tfrac{1}{2} < \alpha = n_A - n_A^0 < \tfrac{1}{2}, \tag{31}$$

$$-\tfrac{1}{2} < \beta = n_B - n_B^0 < \tfrac{1}{2}. \tag{32}$$

That is, when the parameters of the system satisfy the following conditions:

$$n_A^0 - 1 < \frac{U_{AB}(U_{AB} - U_B + 2\varepsilon_B) - 2\varepsilon_A U_B}{2(U_A U_B - U_{AB}^2)} < n_A^0, \tag{33}$$

$$n_B^0 - 1 < \frac{U_{AB}(U_{AB} - U_A + 2\varepsilon_A) - 2\varepsilon_B U_A}{2(U_A U_B - U_{AB}^2)} < n_B^0, \tag{34}$$

the occupation numbers (n_A^0, n_B^0) minimize the energy $E(n_A, n_B)$.

One loose end in the above discussions is that we have assumed the minimal occupation numbers are nonzero. If one of the occupation numbers is zero, then it means that our ground state is not stable due to the mutual interactions between different species. To get the stability condition for the uniform ground state, we need to diagonalize the interaction terms, namely, the following quadratic form:

$$U(n_A, n_B) = \tfrac{1}{2}(U_A n_A^2 + U_B n_B^2 + 2 U_{AB} n_A n_B). \tag{35}$$

The eigenvalues of this quadratic form are

$$n_{\pm} = \tfrac{1}{4}\left[(U_A + U_B) \pm \sqrt{(U_A + U_B)^2 + 4(U_{AB}^2 - U_A U_B)}\right]. \tag{36}$$

Therefore, n_- may become negative; if so, the interaction manifold is saddlelike and one cannot really minimize the ground-state energy with two nonzero occupation numbers. Thus, in one spatial region, one of the species must have zero occupation. In other words, the ground state of the system must be phase separated when the following condition is satisfied:

$$U_A U_B \lesssim U_{AB}^2. \tag{37}$$

This condition (37) for phase separation is analogous to that of an ordinary two-component BEC (without being loaded into an optical lattice) [19–21]. In the case when the Wannier functions are the same for both species, this condition is reduced precisely to that in the absence of the optical lattice.

IV. PHASE TRANSITION TO A SUPERFLUID

In this section, to study possible phase transitions, we are going to present a mean-field theory based on the ground state developed in the preceding section. The hopping processes correspond to moving bosons from one site to another. This process allows bosons at different sites to communicate with each other and finally they conspire to establish macroscopic coherence under appropriate conditions. In this way

the system can enter a superfluid state with indefinite filling of bosons at each site.

To study phase transitions, it is more convenient to start with the grand canonical ensemble, so we add the chemical potential term, $-\mu_A \Sigma_m n_{mA} - \mu_B \Sigma_m n_{mB}$, to the Hamiltonian. For simplicity, we consider the homogeneous case, with $\epsilon_{mA} = 0$ and $\epsilon_{mB} = 0$. (When a slowly varying trapping potential is included, we only need to shift locally $\mu_{A/B} \rightarrow \mu_{A/B} - \epsilon_{m,A/B}$ in the final formulas.)

The consistent mean-field theory we shall use corresponds to the following decomposition of the hopping terms:

$$b_m^\dagger b_n \approx \langle b_m^\dagger \rangle b_n + b_m^\dagger \langle b_n \rangle - \langle b_m^\dagger \rangle \langle b_n \rangle = \phi(b_m^\dagger + b_n) - \phi^2, \tag{38}$$

where $\phi = \langle b_m^\dagger \rangle = \langle b_n \rangle$ is the superfluid order parameter. In the case at hand, we have taken the order parameter to be real. In this decomposition, the higher-order fluctuations $(b_m^\dagger - \phi)(b_n - \phi)$ have been neglected. It reflects the fact that in the ground-state energy corrections we neglect the correlation energy. Generally speaking, this process will increase the energy, and therefore the free energy as well, of the system; however, when the system parameters satisfy certain conditions, this process will not cost any free energy or even will lower the free energy of the system. This signals the occurrence of a phase transition. Therefore, the vanishing free-energy correction due to the hopping process should give us the phase boundary. In the following, we shall determine the phase boundary using second-order perturbation theory.

The resulting mean-field version of the hopping Hamiltonian can be written as

$$H^{eff} = \sum_m H_m^{eff} = -zJ \sum_m \left[\phi_A(b_{mA}^\dagger + b_{mA}) + \phi_B(b_{mB}^\dagger + b_{mb}) - (\phi_A^2 + \phi_B^2) \right]. \tag{39}$$

Here z is the number of nearest-neighbor sites. Since it is a single sum over all lattice sites, we drop the site index from now on.

The first-order correction to free energy vanishes, due to the fact that the ground state is a product of number eigenstates at each site, and thus the average of an annihilation or creation operator is just zero. The second-order correction to free energy is given by the following well-known expression:

$$E_g^{(2)} = \sum_{n \neq g} \frac{|\langle g|H_m^{eff}|n\rangle|^2}{E_g^{(0)} - E_n^{(0)}}, \tag{40}$$

where $|n\rangle = |n_A, n_B\rangle$ denotes the unperturbed state with n_A and n_B atoms for each species, respectively. Correspondingly, $|g\rangle = |n_A^0, n_B^0\rangle$ is the ground state and the occupation numbers are given by Eqs. (33) and (34). A straightforward calculation gives the ground-state free energy up to second order as follows:

$$E_g^{(0)} + E_g^{(2)} = J^2 z^2 \phi_A^2 \left[\frac{n_A^0}{-\mu_A + U_A(n_A^0 - 1) + U_{AB} n_B^0} \right.$$

$$\left. + \frac{n_A^0 + 1}{\mu_A - U_A n_A^0 - U_{AB} n_B^0} \right]$$

$$+ J^2 z^2 \phi_B^2 \left[\frac{n_B^0}{-\mu_B + U_B(n_B^0 - 1) + U_{AB} n_A^0} \right.$$

$$\left. + \frac{n_B^0 + 1}{\mu_B - U_B n_B^0 - U_{AB} n_A^0} \right] + Jz(\phi_A^2 + \phi_B^2). \tag{41}$$

Here the last two terms are the zeroth-order contribution from the Hamiltonian (39).

Therefore, the phase boundaries between the Mott insulator and the superfluid for species A and B, respectively, are given by the following conditions:

$$1 + Jz \left[\frac{n_A^0}{-\mu_A + U_A(n_A^0 - 1) + U_{AB} n_B^0} \right.$$

$$\left. + \frac{n_A^0 + 1}{\mu_A - U_A n_A^0 - U_{AB} n_B^0} \right] = 0,$$

$$1 + Jz \left[\frac{n_B^0}{-\mu_B + U_B(n_B^0 - 1) + U_{AB} n_A^0} \right.$$

$$\left. + \frac{n_B^0 + 1}{\mu_B - U_B n_B^0 - U_{AB} n_A^0} \right] = 0. \tag{42}$$

Solving above equations yields the phase boundaries

$$\mu_A = \mu_A^\pm \equiv \tfrac{1}{2} [2 U_{AB} n_B^0 + U_A(2 n_A^0 - 1) - Jz$$

$$\pm \sqrt{U_A^2 - 2 U_A Jz(2 n_A^0 + 1) + (Jz)^2}], \tag{43}$$

$$\mu_B = \mu_B^\pm \equiv \tfrac{1}{2} [2 U_{AB} n_A^0 + U_B(2 n_B^0 - 1) - Jz$$

$$\pm \sqrt{U_B^2 - 2 U_B Jz(2 n_B^0 + 1) + (Jz)^2}]. \tag{44}$$

When the chemical potential μ_A is in the region

$$\mu_A^- < \mu_A < \mu_A^+, \tag{45}$$

the free-energy correction due to the tunneling events of species A is positive and thus the Mott insulator is the stable ground state. A similar result is valid for species B. When the interspecies interaction U_{AB} and the intraspecies repulsions $U_{A/B}$ satisfy the condition (37), we see that the mutual interactions and nonzero occupation for the other species indeed modify the phase boundary for both species. When the interspecies interaction is strong enough to make the system phase separated, the system can be viewed as two totally independent single species in the optical lattice.

V. SCHEMATIC PHASE DIAGRAM

Now we are in the position to discuss the phase diagram of the system. Normally for the one-species boson-Hubbard model, which is known to be the model for one-species BEC in an optical lattice [16], the phase diagram is drawn in $U - \mu$ space (see, e.g., Fig. 2 in Ref. [7]). From Eqs. (43) and (44), it is easy to see that if $U_{AB} = 0$, i.e., there are no interspecies interactions, then the position of the lobe $L_{A/B}$ will be the same as for the single-species case. This motivates us to explore the $U_{A/B} - \mu_{A/B}$ space to make a schematic phase diagram for a two-species BEC in optical lattices; namely, we make the two two-dimensional $U_A - \mu_A$ and $U_B - \mu_B$ spaces coincident with each other. Then the two-component system is represented by *two* points A and B, with coordinates (U_A, μ_A) and (U_B, μ_B), respectively, in this space. The phase boundaries described by Eqs. (43) and (44), respectively, are represented by two hyperbolas, labeled L_A and L_B, in this space (with other parameters fixed). Some examples are shown in Fig. 1, where the axes in each diagram are either μ_A versus U_A or μ_B versus U_B.

According to Eqs. (43) and (44), the positions of L_A and L_B depend on the occupation numbers $n_A^{(0)}$ and $n_B^{(0)}$: Compared to the case with $U_{AB} = 0$, the effect of the interspecies interaction U_{AB} is to shift L_A or L_B in the vertical (i.e., $\mu_{A/B}$) direction, by an amount of $U_{AB} n_{B/A}^{(0)}$ that depends on the density of the other species. Unless $n_A^{(0)} = n_B^{(0)}$, the amount of the shift is different for L_A and L_B. Therefore, the shape and the size of each phase boundary $L_{A/B}$ are the same as the single-species case, independent of U_{AB}. An interesting consequence is that the horizontal position of the tip (i.e., the least value of $U_{A/B}$) of each lobe L_A or L_B, determined by the condition $\mu_{A/B}^+ = \mu_{A/B}^-$, is independent of the interspecies interaction U_{AB}, and thus it is independent of the occupation number of the other species too. Indeed, the tip of the lobe for species A (or B) is determined by the requirement that the expression under the square root in Eq. (43) should vanish, so they are given by

$$\left(\frac{U_{A/B}}{Jz} \right)_c = 2 n_{A/B}^0 + 1 + \sqrt{(2 n_{A/B}^0 + 1)^2 - 1}, \tag{46}$$

which is the same as for the single-species boson-Hubbard model. (It is worth noting that this result is valid even if the hopping integrals are not equal, $J_A \neq J_B$: The only change we need to make is to scale $U_{A/B}$ by the corresponding hopping parameter $J_{A/B} z$.)

Keeping the above observations in mind, we see that there are three possibilities for the relative positions of lobes L_A and L_B in $U_{A/B}$-$\mu_{A/B}$ space.

(1) When $n_A^{(0)} = n_B^{(0)}$, the lobes L_A and L_B coincide with each other, as shown in Fig. 1(a). The space is divided into two regions, labeled as SF (superfluid) and MI (Mott insulator), respectively. The region MI is enclosed by both lobes, and SF is outside both of them. When the representative point A or B falls in SF, then the corresponding species A (or B) is in the superfluid phase. The meaning of region MI is similar.
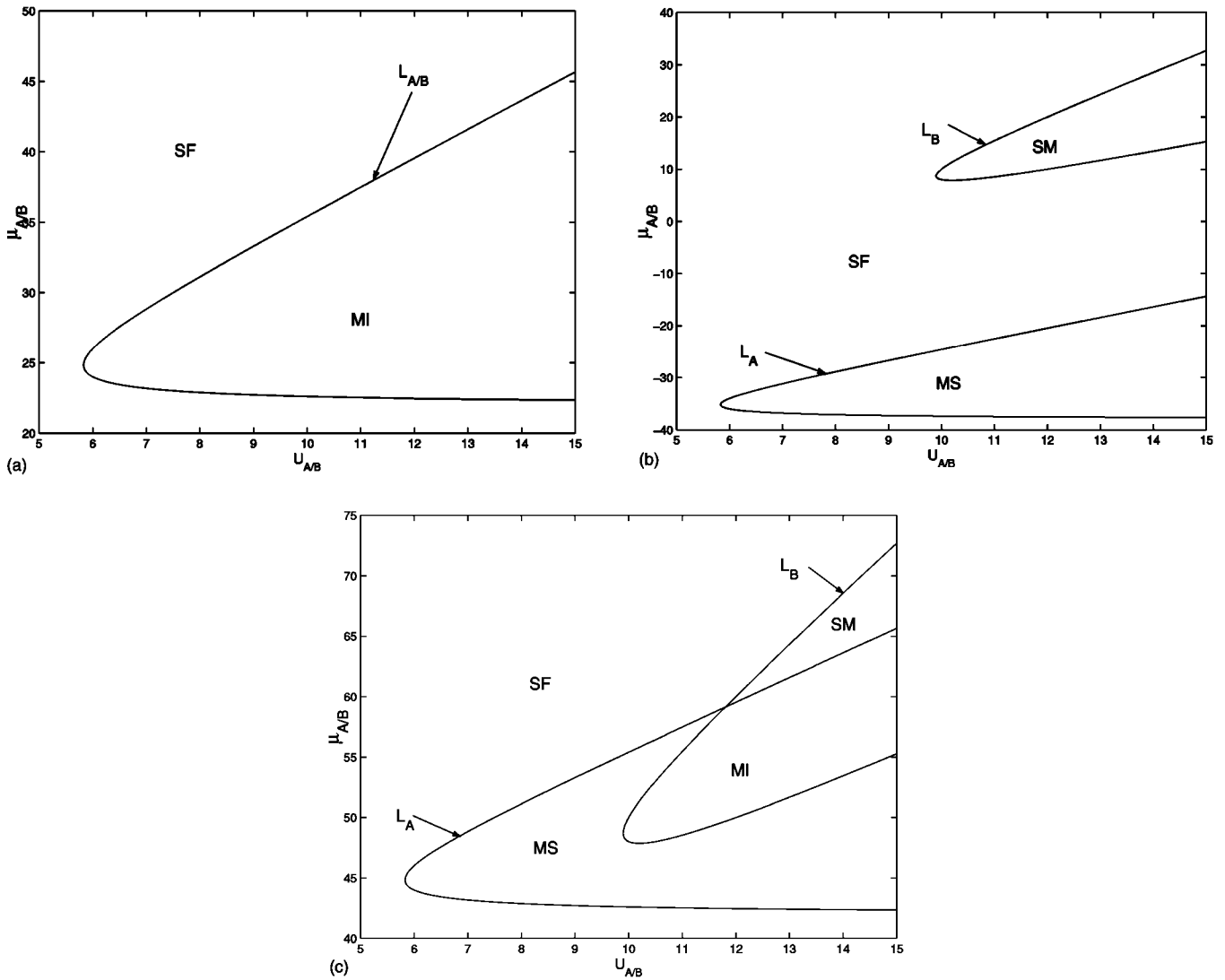
FIG. 1. The schematic phase diagram of the two-component boson-Hubbard model. The axes are either μ_A versus U_A or μ_B versus U_B, all in units of Jz. [The system should be represented by two points A and B with coordinates (U_A,μ_A) and (U_B,μ_B), respectively.] The phase boundary for species A and B is given by two curves L_A and L_B. Depending on their relative positions, L_A and L_B may divide the diagram into two, three, or four regions, etc. Some examples are shown here with: (a) $n_A^0=n_B^0=1$, $U_{AB}=10Jz$; (b) $n_A^0=1$, $n_B^0=2$, $U_{AB}=-10Jz$; and (c) $n_A^0=1$, $n_B^0=2$, $U_{AB}=10Jz$. The meaning of the regions, labeled SF, SM, MS, and MI, and how to use the phase diagram are explained in detail below Eq. (46).

(2) When $n_A^{(0)}<n_B^{(0)}$ and $U_{AB}<0$, the lobes L_A and L_B do not intersect at all. [One such case is shown in Fig. 1(b).] This is because the lobe L_A is lower than L_B, and the downward shift of L_A is bigger than that of L_B. Therefore, as shown in Fig. 1(b), there are three regions in the diagram, labeled as SF, MS (Mott insulator superfluid), and SM (superfluid-Mott insulator). The region, say, SM is outside L_A and inside L_B. The meaning of SM is that when point A falls in it, species A is in the superfluid phase, while if point B is in this region, species B is in the Mott insulator phase. And vice versa for the region MS.

(3) When $n_A^{(0)}<n_B^{(0)}$ and $U_{AB}>0$, the lobes L_A and L_B may or may not intersect, depending on the values of U_{AB}, n_A^0 and n_B^0. In this case, the lower lobe L_A is always shifted upward more than the upper lobe L_B; so with fixed $n_{A/B}^{(0)}$, if U_{AB} is larger enough, L_A can intersect with L_B. One ex-

ample with such intersection is shown in Fig. 1(c), where there are four regions in the diagram, labeled as SF, MS, SM, and MI. The meaning of the labeling is the same as in the previous cases. If L_A does not intersect with L_B, the situation is similar to the above case (2).

Recalling that the system is represented by *two* separate points A and B, which generically can be anywhere in the diagram except respecting the constraint (37), we conclude that depending on the parameters, the following three phases are possible: (1) both species A and B are in the superfluid phase; (2) one of the species is in the superfluid phase, while the other is in the Mott-insulator phase; (3) both species are in the Mott-insulator phase.

An interesting question arises when the system is a mixture of the superfluid phase for one component and and Mott insulator phase for the other: Which phase corresponds to the larger scattering length? From the diagrams one can see that

there is *no universal* answer to this question. In other words, the species with a larger scattering length can be either in the superfluid phase or the other way around, depending on other parameters of the system.

VI. CONCLUSIONS AND DISCUSSIONS

In this paper, we have analytically studied the quantum phase transition between a superfluid and the Mott insulator for a multicomponent BEC system in an optical lattice. Theoretically, this is a generalization of the well-studied case of the boson-Hubbard model in the condensed-matter literature. Experimentally, the observation of such a quantum phase transition is accomplished by loading a one-component atomic Bose-Einstein condensate into an artificial optical lattice. These motivate us to study the role of the interspecies interactions in the QPT for the multicomponent cases.

In the first part of the paper, we have generalized the single-species boson-Hubbard model to the multicomponent case with most general interactions. To be precise, we have reduced our general boson-Hubbard model to the two- and three-component cases under appropriate conditions.

Starting with the two-component boson-Hubbard model, we developed a mean-field theory to study the quantum phase transition. Depending on interspecies interactions, the system may be in different ground states. If the repulsion between two species is not very strong, the two species can coexist; namely, the system is miscible. However, if the repulsion is sufficiently strong, the two species may become immiscible, and the ground state will demonstrate the behavior of phase separation; that is, two species of Mott insulator will stay in separate spatial regions. After turning on the tunneling terms, the ground-state free energy will get corrections from tunneling. We calculated the free-energy corrections up to second order and determined the boundary be-

tween the gain and loss in free energy. We found that the interspecies interactions indeed can change the position of the phase boundary for the Mott insulator. However, the interspecies interactions cannot change the tip, i.e., the critical $U_{A/B}$ value, of the Mott-insulator lobes. The phase diagram of the two-component boson-Hubbard model also demonstrates a rich structure. From our analytical treatment, we conclude that the following three different phases are possible: (1) Both species A and B are in the superfluid phase; (2) one of the species is in the superfluid phase, while the other is in the Mott insulator phase; and (3) both species are in the Mott-insulator phase;

Finally, several further remarks are in order.

(1) Above results for a two-component system can be directly generalized to the spinor BEC and other systems with more components.

(2) One can check without difficulty that there is indeed an energy gap in the excitation spectrum of the Mott insulator. The gap at zero momentum is determined by the intraspecies interactions $U_{A/B}$ and is independent of the interspecies interactions U_{AB}. Right at the phase transition, due to the gain of tunneling, the energy gap closes. Therefore, the system becomes compressible (or gapless) and therefore is in a superfluid phase.

(3) In this paper, our studies of the phase diagram for the multispecies boson-Hubbard model have been restricted in the case where the Josephson-type tunneling term can be neglected. Under certain experimental conditions, such terms would be dominant and the physics is significantly changed. The results for this case will be published somewhere else [22].

[1] S.L. Sondhi *et al.*, Rev. Mod. Phys. **69**, 315 (1997).

[2] S. Sachdev, *Quantum Phase Transitions* (Cambridge University Press, New York, 1999).

[3] M. Wallin *et al.*, Phys. Rev. B **49**, 12 115 (1994).

[4] D.S. Fisher and M.P.A. Fisher, Phys. Rev. Lett. **61**, 1847 (1988); M.P.A. Fisher *et al.*, Phys. Rev. B **40**, 546 (1989).

[5] K. Sheshadri *et al.*, Europhys. Lett. **22**, 257 (1993).

[6] J.K. Freericks and H. Monien, Europhys. Lett. **26**, 545 (1994).

[7] D. van Oosten, P. van der Straten, and H.T.C. Stoof, Phys. Rev. A **63**, 053601 (2001).

[8] S.A. Grigera *et al.*, Science **294**, 329 (2001).

[9] M. Greiner *et al.*, Nature (London) **415**, 39 (2002).

[10] T.L. Ho and V.B. Shenoy, Phys. Rev. Lett. **77**, 2595 (1996).

[11] T.L. Ho, Phys. Rev. Lett. **81**, 742 (1998).

[12] H.T.C. Stoof, E. Vliegen, and U. Al Khawaja, Phys. Rev. Lett.

87, 120407 (2001); U. Al Khawaja and H.T.C. Stoof, Nature (London) **401**, 918 (2001).

[13] Fei Zhou, e-print cond-mat/0108437, and references therein.

[14] For a review, see J. R. Anglin and W. Ketterle, in *Bose-Einstein Condensation of Atomic Gases*, special issue of Nature (London) **416**, 206 (2002).

[15] D.M. Stamper-Kurn and W. Ketterle, e-print cond-mat/0005001.

[16] D. Jaksch *et al.*, Phys. Rev. Lett. **81**, 3108 (1998).

[17] C.J. Myatt *et al.*, Phys. Rev. Lett. **78**, 586 (1997).

[18] J. Cirac *et al.*, Phys. Rev. A **57**, 1208 (1998).

[19] J.P. Burke *et al.*, Phys. Rev. A **55**, 2511 (1997).

[20] H.M.J.M. Boesten *et al.*, Phys. Rev. A **55**, 636 (1997).

[21] P. Ao and S.T. Chui, Phys. Rev. A **58**, 4836 (1998).

[22] Guang-Hong Chen and Yong-Shi Wu (unpublished).